MILLIMETER ARRAY
MEMO NO. 15

THE UNIVERSITY OF ARIZONA
TUCSON, ARIZONA 85721

STEWARD OBSERVATORY

March 21, 1984

Dr. Frazer Owen
National Radio Astronomy Observatory
P.O. Box O
Socorro, NM 87801

Dear Frazer:

In an effort to understand the effects of atmospheric turbulence on radio wavelength "seeing", I have written an internal report which deals with the subject. Appendix A of the attached memorandum is a tutorial on atmospheric refractivity fluctuations and the resulting effects on electromagnetic wave propagation. You will find there an explanation of why the centimeter seeing is not much worse than optical seeing. Appendix B presents the published data on the wavelength dependence of Fried's length and predicts the maximum useful sizes of ground-based millimeter arrays. I am also sending copies to Sramek, Clark, and Napier and would appreciate any comments you might have.

If you feel it would be useful for others to see this work, you are welcome to distribute the appendices as a MM-Array Technical Memorandum.

Sincerely,

Bobby

Bobby L. Ulich

nrl

c: Barry Clark
Peter Napier
Richard Sramek

Encl: SMT Technical Memorandum UA-84-3

APPENDIX A

Theory of Electromagnetic Plane Wave Propagation in a Turbulent Medium

The theory of the effects of atmospheric turbulence on the propagation of electromagnetic waves is well-developed for certain cases which encompass a useful range of actual observing conditions (Tatarskii 1971). Energy at very large scales is put into the atmosphere and disturbances cascade down to smaller and smaller scale sizes such that less energy is dissipated by turbulence at smaller scales. The maximum scale size of turbulence L_o for a given path is generally assumed to be either about equal to some significant fraction of the height of the path above the ground (for horizontal paths or short vertical paths) or of the thickness of the atmosphere (for vertical paths through the atmosphere). The minimum scale length ℓ_o is generally taken as a few millimeters. The inertial subrange of turbulent spatial frequencies corresponds to telescope dimensions between ℓ_o and L_o, and most of the results described here (which assume Kolmogoroff turbulence) are strictly valid only in this regime. The simplest model assumes that the atmosphere is <u>lossless</u> (non-absorbing), and that the refractive index of the air is not frequency dependent, but changes with time only due to temperature fluctuations. This is certainly not true in practice but in fact for many applications these crude assumptions do not cause significant errors (especially at optical frequencies). For instance, at very long (decimeter to centimeter) and for very short (optical) wavelengths the absorption of the atmosphere is very small and does not vary much with the water vapor content. However, at intermediate (sub-millimeter) wavelengths, wet air is much lossier than dry air, and both the real and the imaginary parts of the refractive index will also vary with humidity. While including these loss

effects is possible by extending the simple theory (Gurvich 1968 and Izyumov 1968), I will not attempt to do so here. Instead, I will assume that the atmosphere is lossless (i.e., that the imaginary part of the index of refraction is zero) and that the real part of the refractivity varies with pressure, temperature, and humidity in a slowly varying fashion with wavelength.

A1. INDEX OF REFRACTION OF AIR

The real part of the index of refraction of moist air at radio frequencies away from O_2 and H_2O resonance lines is given by the expression (Smith and Weintraub 1953)

$$n = 1 + 10^{-6}[77.6\ P/T - 6e/T + 3.75 \times 10^5 e/T^2] \qquad (A1)$$

where P is the total air pressure (mb), T is the absolute temperature (K), and e is the partial pressure of water vapor (mb). The coefficients of the water vapor terms are generally good to within $\frac{1}{2}$ % for frequencies up to 72 GHz (Bean 1962) since the atmospheric dispersion is very small except at resonant frequencies of O_2 and H_2O (Liebe and Hopponen 1977). From Equation A1 we can see that variations in T, P, or e will cause n to vary. In practice, variations in T and e are most important on relatively short time scales (< 1 day) and rapid variations in P are generally neglected. The electrical path length correction is given by

$$\Delta R = \int_0^R (n-1)ds \qquad (A2)$$

where R is the total path length. Typical values of ΔR for a vertical path

through the atmosphere are 2.2 to 2.7 m (Pandey and Kakar 1983). Multifrequency microwave sky emission monitors can determine ΔR with an accuracy of about 5 mm. Humidity variations can cause variations in ΔR as large as about 30 cm for a sea-level site. The excess path length (which is essentially independent of frequency in the radio range) due to water vapor is about equal to 6.5W where W is the precipitable H_2O vapor (in cm) along the line of sight (Hogg et al. 1981). The vertical excess path length due to dry air is given (in cm) by 0.2276 (P-e). The surface water vapor pressure e in mb is approximately related to the precipitable water vapor W (in cm) by e = 0.98 W and to the specific humidity Q (g/m^3) by

$$e = TQ/217 \qquad \text{(A3)}$$

(Friehe et al. 1975). The total excess path length is therefore approximately given by

$$\Delta R \text{ (cm)} = 0.2276\ P_S + 6.277\ W\ . \qquad \text{(A4)}$$

where P_S is the total air pressure (mb) at the surface (Hogg et al. 1981).

The dominant effect of atmospheric absorption on the scintillation spectral density function is an enhancement at the low frequency end (<0.03 Hz) (Filho et al. 1983). Including absorption has no effect on the shape of the temporal power spectrum of phase fluctuations (Ott and Thompson 1978). Amplitude fluctuations are due both to forward scattering and to variations in the absorption. According to Izyumov (1968), including absorption has the following effects:

(1) The magnitude of the phase fluctuations is essentially unaffected except very near the maximum absorption frequencies of resonant lines where there is a very small increase in phase variations. This has significant implications concerning sub-millimeter interferometry. Basically it means that the atmospheric excess path length is virtually independent of radio frequency. Measurements using low-frequency radio interferometers can therefore be used to predict the performance of high-frequency interferometers.

(2) Increasing the absorption coefficient results in a decrease in the variance of the logarithm of the ratio of the signal amplitude to its mean value.

(3) Increasing the humidity along the propagation path decreases the relative signal amplitude fluctuations compared to the level of fluctuations in the absence of absorption. This decrease is larger near absorption lines and for larger scale sizes of inhomogeneities (lower frequency time variations). According to Armand et al. (1971) this reduction in fading is only valid in the geometrical optics zone (where $(R\lambda)^{1/2} << L_0$) and is significant only when lens effects and absorption effects are comparable in magnitude.

Increasing the receiving aperture dimensions will only reduce the amplitude variations caused by variations in absorption when the aperture dimension exceeds the outer scale of turbulence L_0 (Gurvich 1968). Clifford and Strohbehn (1970) have also shown that the results derived under the assumption that the wavelength λ is much less than the inner scale of turbulence ℓ_0 are also valid

when $\lambda \geq \ell_0$.

In summary, the effects of absorption are negligible on the phase fluctuations and are rather small on the amplitude fluctuations. In some cases the very low frequency amplitude variations are increased by the effects of absorption. However, direct measurements near λ = 1 mm show a significant decrease in the high-frequency amplitude fluctuations at frequencies near a resonant absorbing H_2O line. In any case, neglecting absorption and using the simple (lossless) model of air will give fairly accurate estimates of signal fading.

The real part of the index of refraction of moist air at optical frequencies (λ = 0.5 micrometers) is given by (Allen 1963)

$$n = 1 + 10^{-6}[79.3\ P/T - 91.5\ e/T] \qquad (A5)$$

and the refractivity hardly changes for the entire visible band. Comparing Equations A1 and A5 we can see that the refractivity of dry air (e = 0) is about 2% smaller at radio than at optical frequencies. However, for significant humidity the radio refractivity is larger than the optical. Rewriting these equations in terms of the more easily measured specific humidity (Equation A3), we get for the radio case

$$n = 1 + 10^{-6}\ [77.6\ P/T - 0.028\ Q + 1728\ Q/T] \qquad (A6)$$

and for the optical case

$$n = 1 + 10^{-6}\ [79.3\ P/T - 0.422\ Q]. \qquad (A7)$$

The term involving Q but not P or T is not surprising since the refractivity is due basically to the number of water molecules in air. Changes in the refractive index of air are not proportional to changes in mass density but rather to number density and the type of gas molecule (Friehe et al. 1975). In general, then, we can write

$$n = 1 + A\,P/T + B\,Q + C\,Q/T \qquad \text{(A8)}$$

where in the radio case

$$A = 7.76 \times 10^{-5}\ K\ mb^{-1} \qquad \text{(A9)}$$

$$B = -2.8 \times 10^{-8}\ g^{-1}\ m^{3}$$

$$C = 1.73 \times 10^{-3}\ K\ g^{-1}\ m^{3}$$

and in the optical case

$$A = 7.93 \times 10^{-5}\ K\ mb^{-1} \qquad \text{(A10)}$$

$$B = -4.22 \times 10^{-7}\ g^{-1}\ m^{3}$$

$$C = 0.$$

A2. TEMPERATURE VARIATIONS

The random air temperature fluctuations are typically 0.1 to 1 K R.M.S. near the ground. A single temperature structure parameter C_T can be determined by measuring the mean-squared temperature differences between two points (1 and 2) which are a distance r apart, and by calculating C_T^2 according to the formula

(Gur'yanov 1980)

$$C_T^2 \equiv \langle (T_1 - T_2)^2 \rangle \, r^{-2/3} \; (K^2 m^{-2/3}) \; . \qquad \text{(A11)}$$

This result is based on the Kolmogoroff theory of turbulence (Kolmogoroff 1961) which predicts a spatial correlation of turbulence which decreases according to the two-thirds power of the spatial separation. The mean-squared temperature variation $\langle \Delta T^2 \rangle$ has a power spectral density per unit bandwidth which varies as $f^{-5/3}$, where f is the frequency in Hz. Most of the energy in this Kolmogoroff spectrum occurs at frequencies between 0.03 and 10 Hz for typical fluctuations over baselines of about a meter, which is appropriate for optical telescopes. Over longer baselines the fluctuations are, of course, much slower. At a height of 15 m above the ground, a typical value of C_T^2 is 10^{-3} $K^2 m^{-2/3}$.

A3. PRESSURE FLUCTUATIONS

The short-time scale atmospheric pressure fluctuations are known to be very small, and at a single point typical R.M.S. fluctuations are on the order of 10^{-2} to 10^{-3} mb (Hill 1978). Therefore, in comparison with the temperature and humidity fluctuations, the effect of pressure fluctuations (which have a relative magnitude of 10^{-5} to 10^{-6}) on refractivity may be neglected (Hill 1978).

A4. HUMIDITY FLUCTUATIONS

The typical R.M.S. specific humidity fluctuations are on the order of a few percent during the day and are generally smaller at night (Gurvich 1968 and Hill 1978). Measurements of the temporal power spectrum show the same Kolmogoroff ($\sim f^{-5/3}$) behavior (Friehe et al. 1975) as do temperature fluctuations.

Therefore we can define a humidity structure parameter C_Q (analogous to the temperature structure parameter C_T) as follows:

$$C_Q^2 = \langle (Q_1 - Q_2)^2 \rangle \, r^{-2/3} (g^2 m^{-20/3}). \qquad \text{(A12)}$$

The temperature and humidity fluctuations are not independent but can be strongly correlated, as has been shown experimentally and theoretically by Friehe et al. (1975), who measured correlation coefficients with magnitudes of 0.8 in maritime boundary layers. Apparently the humidity fluctuation caused by density variations follows the temperature fluctuation. Therefore we must consider how this correlation affects the fluctuations in refractivity. The refractivity variance and power spectrum depend on the relative contributions of the temperature spectrum, humidity spectrum, and temperature-humidity cospectrum. The sign of the temperature-humidity correlation is equal to the product of the signs of the surface vertical fluxes of heat and moisture (Friehe et al. 1975), and a lack of correlation may exist where either flux is zero. Whenever warm, dry air lies above cold, moist air (such as near the ground at night), the cospectrum is expected to be negative. In this case the covariance subtracts from the refractive index variance caused by only temperature fluctuations. To quote Friehe et al.:

> "Humidity fluctuations may also be important over land in cases where there is a significant moisture flux from the ground. In some locations it may be possible that refractive-index fluctuations may be significantly decreased (compare to temperature-driven variations only), owing to the negative temperature-humidity correlation."

Since both the temperature and humidity power spectra are of the Kolmogoroff type, so are the temperature-humidity cospectrum and the net refractivity spectrum.

We can define a cospectrum temperature-humidity structure parameter C_{TQ} (Wyngaard et al. 1978) such that

$$C_{TQ} \equiv \langle (T_1 - T_2)(Q_1 - Q_2) \rangle \, r^{-2/3} (K \; g \; m^{-11/3}). \tag{A13}$$

which is analogous in form to C_T^2 and to C_Q^2, but which can be positive or negative. The (signed) correlation coefficient r_{TQ} is simply given by

$$r_{TQ} \equiv \frac{C_{TQ}}{C_T C_Q} \; . \tag{A14}$$

A5. REFRACTIVE INDEX STRUCTURE PARAMETER

Similarly, the refractive index structure parameter C_n is defined by

$$C_n^2 \equiv \langle (n_1 - n_2)^2 \rangle \, r^{-2/3} \; (m^{-2/3}) \tag{A15}$$

where the index of refraction n is given by Equation A8. We can relate C_n^2 to C_T^2, C_Q^2, and C_{TQ} through differentiating Equation A8 and finding the mean-squared refractive index fluctuation. First, we write the total differential Δn as the sum of the partial derivatives:

$$\Delta n = \frac{\partial n}{\partial T} \Delta T + \frac{\partial n}{\partial P} \Delta P + \frac{\partial n}{\partial Q} \Delta Q \; . \tag{A16}$$

Next we find the square of the differential:

$$(\Delta n)^2 = \left(\frac{\partial n}{\partial T}\right)^2(\Delta T)^2 + \left(\frac{\partial n}{\partial P}\right)^2(\Delta P)^2 + \left(\frac{\partial n}{\partial Q}\right)^2(\Delta Q)^2 \qquad \text{(A17)}$$

$$+ 2\left(\frac{\partial n}{\partial T}\right)\left(\frac{\partial n}{\partial P}\right)(\Delta T)(\Delta P)$$

$$+ 2\left(\frac{\partial n}{\partial T}\right)\left(\frac{\partial n}{\partial Q}\right)(\Delta T)(\Delta Q)$$

$$+ 2\left(\frac{\partial n}{\partial P}\right)\left(\frac{\partial n}{\partial Q}\right)(\Delta P)(\Delta Q) .$$

As discussed previously, the pressure fluctuations are found in practice to be so small that they do not contribute significantly to the refractive index fluctuations. Therefore, we can now make the isobaric approximation and assume that $\Delta P = 0$. This considerably simplifies Equation A17 and we can now rewrite it and take the time average as follows:

$$\langle(\Delta n)^2\rangle \approx \left(\frac{\partial n}{\partial T}\right)^2\langle(\Delta T)^2\rangle + 2\left(\frac{\partial n}{\partial T}\right)\left(\frac{\partial n}{\partial Q}\right)\langle(\Delta T)(\Delta Q)\rangle \qquad \text{(A18)}$$

$$+ \left(\frac{\partial n}{\partial Q}\right)^2\langle(\Delta Q)^2\rangle$$

From Equation A8 we can approximately evaluate the two partial derivatives in terms of simple parameter means (neglecting second order terms), and we get

$$\frac{\partial n}{\partial T} \approx \frac{-(A\langle P\rangle + C\langle Q\rangle)}{\langle T\rangle^2} = a \qquad \text{(A19)}$$

and

$$\frac{\partial n}{\partial Q} \approx B + C/\langle T\rangle = b. \qquad \text{(A20)}$$

Now we can simplify Equation A18 by substitution to get

$$\langle(\Delta n)^2\rangle \approx a^2\langle(\Delta T)^2\rangle + 2ab\langle(\Delta T)(\Delta Q)\rangle + b^2\langle(\Delta Q)^2\rangle \qquad (A21)$$

which is accurate to a few tenths of one percent (Hill 1978). This equation says the variance of refractive index about its mean value is equal to the weighted sum of the variances of the temperature and humidity variances plus the cross correlation term. Since all these terms have Kolmogoroff spatial and temporal spectra (Wyngaard et al. 1978), we can also write

$$C_n^2 \approx a^2C_T^2 + 2abC_{TQ} + b^2C_Q^2 \qquad (A22)$$

which is the desired result. When C_{TQ} is negative the cross term can sometimes be larger in magnitude than both the C_T^2 and the C_Q^2 terms and can result in lower values of Cn^2 (i.e., better seeing) than for dry air alone (Friehe et al. 1975). In other situations the cross term is positive and increases Cn^2 (i.e., poorer seeing). This implies that radio seeing (due to temperature and humidity fluctuations) can be better or worse than optical seeing (essentially due to temperature fluctuations only). There are no statistical data so far to indicate how important this effect is for existing radio interferometers, but it is interesting to contemplate selecting a site to minimize C_n^2 near the ground based upon significantly negative values of C_{TQ}.

Near the ground C_n^2 is a maximum and is typically 10^{-15} $m^{-2/3}$ at optical wavelengths (Roddier 1981) at night but is much larger during the day. According to Fante (1980), at optical wavelengths and at altitudes from 3 to 20 km,

$$C_n^2 \approx 2.7 \times 10^{-16}\left[3\langle V^2\rangle (h/10)^{10} e^{-h} + e^{-h/1.5}\right] m^{-2/3} \qquad \text{(A23)}$$

where h is the height above sea level (in km) and V is the wind speed in m/s. At altitudes below 4 km, C_n^2 for microwave frequencies may be as much as a factor of 10 or more greater than optical values (Fante 1980 and Thompson et al. 1980) because of the significant humidity term in the radio refractivity equation. Above 4 km altitude, microwave and optical values of C_n^2 agree fairly well, and Barletti et al. (1977) have confirmed that C_n^2 above 4 km is nearly independent of site. Thus the high altitude component of atmospheric seeing is essentially independent of wavelength and site.

Seeing differences at optical wavelengths are therefore mainly due to local ground convection and orographic disturbances plus thermal disturbances due to the telescope and its surrounding equipment. At the Multiple Mirror Telescope on Mt. Hopkins the median nighttime value of the atmospheric factor $\int_0^\infty C_n^2(h)dh$ is about 7×10^{-13} $m^{1/3}$. Integrating Equation A23 from 3 km to 24 km altitude we get $\int_{3km}^{24km} C_n^2(h)dh \approx 3 \times 10^{-13} m^{1/3}$ which implies an average image FWHM of 0.6 arc seconds at λ = 0.5 micrometers wavelength as a fundamental statistical limit for long exposures using ground-based telescopes. Therefore at the MMT and at other observatories the bulk of the contribution to the turbulent seeing integral is (on the average) from the lowest few kilometers of atmosphere.

A6. FRIED'S LENGTH

The phase fluctuations of an initially plane wave propagating through the atmosphere are in most cases of interest determined by a single parameter, called Fried's transverse phase coherence length r_0. According to Fried (1967a

and Fried and Mevers 1974)

$$r_o = 0.185\,\lambda^{6/5}\left(\int_0^R C_n^2(s)ds\right)^{-3/5} \qquad \text{(A24)}$$

where r_o, the wavelength λ, and the total path length R are in meters. If C_n^2 is constant over a horizontal path,

$$r_o = 0.185\,\lambda^{6/5}\,(\langle C_n^2\rangle R)^{-3/5}\,. \qquad \text{(A25)}$$

The R.M.S. phase variation over a circular aperture of diameter r_o is 1.04 radians (Fried 1965) with no tilt correction. Therefore the R.M.S. phase variation over an aperture of diameter D is given by

$$\begin{aligned}\sigma_D &= 1.04\,(D/r_o)^{5/6} \\ &= 4.24\,D^{5/6}\,\lambda^{-1}\,(\langle C_n^2\rangle R)^{1/2}\ \text{(radian)}.\end{aligned} \qquad \text{(A26)}$$

If the tilt were removed, the R.M.S. phase error over a circular aperture of diameter r_o would be only 0.375 radian (= $\lambda/17$) (Greenwood and Fried 1976), and the R.M.S. phase error is one radian for a circular aperture of diameter $D = 3.4\ r_o$ when wave-front tilt is removed (Fried 1965). Similarly, the R.M.S. phase difference between two points r_o apart is 2.62 radians (Fried 1965), and

$$\begin{aligned}\sigma_r &= \langle(\phi_1 - \phi_2)^2\rangle^{1/2} \\ &= 2.62\,(r/r_o)^{5/6}\ \text{(radian)} \\ &= 10.7\,r^{5/6}\,\lambda^{-1}\,(\langle C_n^2\rangle R)^{1/2}\ \text{(radian)}.\end{aligned} \qquad \text{(A27)}$$

Equation A27 is strictly valid for values of $r > [\lambda R]^{1/2}$ (the near field) but it holds reasonably well (the R.M.S. phase error is reduced by $2^{-1/2}$) even if

$r < [\lambda R]^{1/2}$ (the far field). σ_r will be reduced very slowly by integration as $(\text{time})^{-1/6}$ since most of the phase noise is due to variations larger than the baseline (Sutton et al. 1982). Of course for times longer than the outer scale of turbulence divided by the wind speed along the baseline the phase noise will be uncorrelated. Wave-front compensating optics can be quite effective even if the size of the correcting segments is larger than r_o. Greenwood and Fried (1976) found that subapertures of diameter 1.85 r_o could correct the phase errors to $\lambda/10$ R.M.S. if they are individually moved in piston and in tilt. With piston motion only the correcting elements must be less than 0.55 r_o in diameter to achieve the same residual phase error of $\lambda/10$. At low temporal frequencies the power spectrum of phase fluctuations seen by a point detector varies as $f^{-2/3}$ with no overall tilt removal and as $f^{+4/3}$ with tilt removed. At high frequencies the power spectrum of phase (piston) variations (mean squared phase fluctuations) varies as $f^{-8/3}$. Therefore the R.M.S. phase fluctuation per root Hz will vary as $f^{-11/6}$. The intermediate break frequency f_o is approximately given by V/D where V is the wind speed and D is the total aperture diameter. A correction bandwidth of at least 10 f_o is needed for the wave-front corrector to correct most of the atmospheric phase disturbances.

A7. IMAGE BLUR

When the aperture diameter D is much larger than r_o, the image blur caused by atmosphere turbulence will be larger than the diffraction-limited beamwidth (FWHM = $\theta_d = 1.03\lambda/D$) and is given for long time exposures by

$$\theta_0 = 0.995\ \lambda/r_0 \qquad (A28)$$
$$= 5.39\ \lambda^{-1/5}\ (\langle C_n^2 \rangle R)^{3/5}$$

where the coefficient has been derived using the tables in Johnson (1973) and Roddier (1981). The wavelength dependence of θ_0 has been experimentally verified by comparing 10 micrometer imaging resolution with that obtained at 0.55 micrometers wavelength (Boyd 1978). The long-exposure modulation transfer function (MTF) for a plane wave propagating through the atmosphere is given by (Fried 1966 and Barletti et al. 1977):

$$M(r) = \exp\left[-57.4\lambda^{-2}r^{5/3}\int_0^R C_n^2(s)ds\right] \qquad (A29)$$

where F is the telescope focal length, f is the spatial frequency in the image plane, and $r = \lambda F f = |\bar{r}_1 - \bar{r}_2|$. The long-exposure point spread function ("seeing disk") is just the Fourier Transform of this MTF. This image blurring is partly due to rapid image motion, and fast exposures will show an optimized angular resolution θ_{se} of about $0.73\ \theta_0$ if $D \approx 3.8\ r_0$ when $D \gg [\lambda R]^{1/2}$ and if $D \approx 7\ r_0$ for $D \ll [\lambda R]^{1/2}$ (Fried 1966). The number of speckles in a short-exposure image is about $(D/r_0)^2$ (Roddier 1981). Equation A28 shows that the long-exposure image size is slightly wavelength-dependent ($\sim\lambda^{-1/5}$) and radio observations can in principle produce smaller images than at optical wavelengths.

The width of a slit which passes 68% of the light from a seeing disk is $1.35\ \lambda/r_0$ (Fried and Mevers 1974).

A8. IMAGE MOTION

The image motion has a Kolmogoroff power spectral density so that the image motion squared per unit frequency will vary as $f^{-5/3}$ (Greenwood and Fried 1976). Alternately, the image motion per root Hz will vary as $f^{-5/6}$. Letting σ_m be the R.M.S. one-dimensional image motion we get (Tatarskii 1971)

$$\sigma_m = 0.418\ \lambda D^{-1/6}\ r_0^{-5/6} \qquad \text{(A30)}$$
$$= 1.71\ D^{-1/6}\ (\langle C_n^2 \rangle R)^{1/2}\ \text{(radian)},$$

which is valid if $\ell_0 < D < L_0$ and $D \geq (\lambda R)^{1/2}$. Thus the image motion depends on the integrated turbulence and on the telescope diameter D, but not on the wavelength. Comparing Equations A26 and A30 we get

$$\sigma_m = 0.40\ \sigma_D(\lambda/D)\ . \qquad \text{(A31)}$$

The effective full-width at half maximum of an image due to its R.M.S. motion σ_m in each dimension is given by

$$\theta_m = [8\ell n2]^{1/2}\ \sigma_m\ . \qquad \text{(A32)}$$

The observed long exposure FWHM is approximately given by

$$\theta_{obs}^2 \approx \theta_0^2 + \theta_d^2 \approx \theta_{se}^2 + \theta_m^2\ . \qquad \text{(A33)}$$

The <u>isoplanatic angle</u> is the angle within which the image motion of distant sources is correlated, and it is given by (Loos and Hogge 1979)

$$\theta_i = 0.0581\ \lambda^{6/5}\ \left(\int_0^R C_n^2(s)\ s^{5/3}\ ds\right)^{-3/5} \qquad \text{(A34)}$$

$$= 0.105\ \lambda^{6/5}\ (\langle C_n^2 \rangle R^{8/3})^{-3/5}\ .$$

Typical values of the isoplanatic angle at optical wavelengths are about five arc seconds (Loos and Hogge 1979, Woolf 1982, and Pollaine et al. 1979). It is interesting to note that the off-axis antenna gain of a perfect adaptive optics receiver would fall off to 1/e of its peak value at angles equal to the isoplanatic angle (Loos and Hogge 1979). The distance from the observer of the turbulence most dominant in limiting the isoplanatic angle is approximately equal to r_o/θ_i (Young 1974). Inspection of Equation A24 reveals that r_o, and thus σ_D, σ_r, θ_o, σ_m, and θ_m all depend on the integral of C_n^2 over the path. Therefore it does not matter how the turbulence is distributed (whether it is near or far from the observer), but it depends only on the sum of all contributions. Both the isoplanatic angle θ_i and the scintillation (amplitude fading), however, depend on the distance to the turbulence.

A9. SCINTILLATION

The signal phase variations and log-amplitude variations obey Gaussian statistics (Fried 1967a). The amplitude variations are thus said to be log normal. We can linearize the variable and normalize it so that ordinary gaussian statistics may be used by defining a function σ_A such that

$$\sigma_A^2 = \text{Variance}\ [\ell n(A/\langle A \rangle)] \qquad \text{(A35)}$$

where <A> is the time-averaged value of the received field amplitude A. The received power (intensity) depends on the square of the field amplitude, so for small variations, the R.M.S. intensity (irradiance) variation σ_I is given by Fante (1980) as

$$\begin{aligned}\sigma_I &= 2\sigma_A \\ &= 4.38\ \lambda^{-7/12}\left(\int_0^R C_n^2(s)s^{5/6}ds\right)^{1/2} \\ &= 3.23\ \lambda^{-7/12}(\langle C_n^2\rangle R^{11/6})^{1/2}\end{aligned} \tag{A36}$$

if $D < r_0$ (a point detector) and if $L_0 > (\lambda R)^{1/2}$. In the lower atmosphere the outer scale of turbulence L_0 is about equal to one-third the height above ground (Fante 1980). For $D >> r_0$ the intensity variations are considerably reduced and

$$\sigma_I \sim D^{-7/6}\left(\int_0^R C_n^2(s)s^2ds\right)^{1/2} \tag{A37}$$

which is independent of λ (Roddier 1981). If $L_0 < (\lambda R)^{1/2}$ Fante (1980) gives the formula for weak scintillation ($\sigma_I^2 << 1$) as

$$\sigma_I \approx 8.9\ \lambda^{-1}(\langle C_n^2\rangle R L_0^{5/3})^{1/2}. \tag{A38}$$

The wavelength dependence for both cases has been verified experimentally at millimeter wavelengths by Cole et al. (1978). The distance normal to the propagation path over which the amplitude fluctuations are correlated is approximately 0.76 $(\lambda R)^{1/2}$ (Tatarskii 1971 and Fried 1967b), and therefore the scintillation correction angle is $(\lambda/R)^{1/2}$. At short wavelengths σ_I is larger;

i.e., optical scintillation is much worse than tropospheric radio scintillation.

The turbulence far from the receiver is most effective in producing scintillation. At optical wavelengths the scintillation for a ground-based telescope is dominated by turbulence in a layer near 10 km altitude. However, this layer contributes only a small amount to image motion and blurring.

A10. PATH LENGTH VARIATIONS

The electrical path length variations can be found by simply multiplying the phase errors (in radians) by $(\lambda/2\pi)$. For instance, an initially plane wave received by an aperture of diameter D has R.M.S. variations in path length over the aperture of

$$\delta_D = \sigma_D(\lambda/2\pi) = 0.675\, D^{5/6}(\langle C_n^2\rangle R)^{1/2} \qquad \text{(A39)}$$

which is independent of λ. From Equation A39 we can see that enlarging the aperture (larger D) increases the R.M.S. wavefront error over the aperture relative to the mean phase. Similarly, the R.M.S. path difference between two points at a distance r apart is given by

$$\delta_r = 1.70\, r^{5/6}(\langle C_n^2\rangle R)^{1/2} \; . \qquad \text{(A40)}$$

A11. EFFECT OF AIR MASS

For astronomical imaging applications it is of interest to compare the various parameters which are measured at a given air mass A (= sec Z, where Z is

the zenith angle) to what would be measured at the zenith (A = 1) assuming the atmosphere is vertically stratified but uniform horizontally. This is easily done by replacing the upper limit on the turbulence integral R by $R_Z A$ where R_Z is the vertical (zenith) path length. Now we have the following parameter variations:

Excess path length: $\Delta R \sim A$ (A41)

Fried's transverse phase coherence length: $r_0 \sim A^{-3/5}$

FWHM of long time exposure image: $e_0 \sim A^{3/5}$

R.M.S. phase variation over diameter D: $\sigma_D \sim A^{1/2}$

R.M.S. path length variation over diameter D: $\delta_D \sim A^{1/2}$

R.M.S. phase variation between two points r apart: $\sigma_r \sim A^{1/2}$

R.M.S. path length variation between two points r apart: $\delta_r \sim A^{1/2}$

R.M.S. 1-D image motion: $\sigma_m \sim A^{1/2}$

FWHM of image due to motion: $e_m \sim A^{1/2}$

Isoplanatic angle: $e_i \sim A^{-8/5}$

R.M.S. intensity variation: $\sigma_I \sim A^{11/12}$ if $D < r_0$

$\sigma_I \sim A^{3/2}$ if $D \gg r_0$

The theoretical variation of r_0 with airmass has been verified experimentally by Walters et al. (1979).

A12. SUMMARY

The effects of atmospheric turbulence on ground-based imaging depend on the relative dimensions of the telescope aperture D and the transverse phase coherence length r_0. Table A-I summarizes the relative significance of several

measures of image degradation for several regimes corresponding to this relative dimension.

TABLE A-I

ATMOSPHERIC TURBULENCE EFFECTS

Regime	Image Blur Compared to Diffraction	Image Motion	Intensity Scintillation
$D \ll r_0$	Negligible	Large	Large
$D < r_0$	Noticeable	Significant	Significant
$D > r_0$	Significant	Moderate	Noticeable
$D \gg r_0$	Dominant	Small	Negligible

APPENDIX B

The Wavelength Dependence of Fried's Length

The theory of the effects of atmospheric turbulence on electromagnetic wave propagation presented in Appendix A can be tested in a limited fashion by comparing various measurements which have been made at optical and radio wavelengths.

B1. MEASUREMENTS OF FRIED'S LENGTH

At optical wavelengths a number of statistically significant measurements of Fried's length r_0 have been reported. These measurements are generally indirect and depend on observing image size or image motion or both and then inferring r_0 using the equations presented in Appendix A. Table B-I presents these optical data as well as the published radio interferometric phase data converted to median values of Fried's length. In general the values of r_0 determined at optical wavelengths vary significantly with site, time of day, and season (Walters and Kunkel 1981). The daytime values of r_0 can be as much as a factor of two smaller than the nighttime value (Walters *et al.* 1979) due to an increase in the turbulence of the surface boundary layer. In addition, being on a high mountain can increase r_0 by a factor of two or so compared to a low-altitude site. The random variations with time are typically a factor of about 1.4 in r_0 for one standard deviation of a gaussian probability distribution (Fried and Mevers 1974).

The current state of knowledge concerning the best ground-based locations for optical telescopes is succintly described by Walters *et al.* (1979):

> "... during the night, local terrain features are of minor importance and the site quality depends on the integrated turbulence in the middle and upper atmosphere above the site. This is true for mountain locations above the inversion layer. During the day, the best sites have a thin surface boundary layer. The intensity of the optical turbulence within the first few meters of the ground is similar for all sites (on the order of 1×10^{-12} $m^{-2/3}$ at 1 m altitude); but the altitude dependence and hence the effective thickness of the boundary layer above the site depends on the aerodynamics around the terrain feature. A good site emulates a tall tower; a bad site elevates and/or aggravates the planar surface boundary layer."

The radio data in Table B-I are derived from interferometric measures of the phase difference between two separated antennas (σ_r) using Equation A27. In some cases it is not clear whether the phase measurements refer to the zenith or to greater air mass, but here it is assumed that they apply to the zenith. It is not known whether radio "seeing" varies in the same way as optical "seeing", but all indications are that they behave similarly. Thus daytime low-altitude seeing will have values of r_0 a factor of about four smaller than nighttime mountain-top seeing. In addition, the median values of r_0 listed in Table B-I will be exceeded (i.e., better seeing) by a factor of at least 1.4 about 18% of the time.

TABLE B-I

MEASUREMENTS OF FRIED'S LENGTH

Reference	Site	λ	$\langle r_o \rangle$ (m)
Ulich (1984)	Mt. Hopkins, Arizona	0.50 μm	0.12 (night)
Miller and Zieske (1977)	Haleakala, Hawaii	0.50 μm	0.10 (night)
Walters (1981)	New Mexico desert	0.50 μm	0.05
Walters (1981)	New Mexico mountains	0.50 μm	0.08 (night)
Walters (1981)	New Mexico mountains	0.50 μm	0.04 (day)
Dainty and Scaddan (1975)	Mauna Kea, Hawaii	0.52 μm	0.12 (night)
Fried and Mevers (1974) and Fried (1977)	Flagstaff and Kitt Peak, Arizona	0.55 μm	0.08 (night)
Bieging et al. (1984)	Hat Creek, California	3.5 mm	1700
Sramek (1983)	VLA, New Mexico	1.33 cm	15,000
Hinder (1970)	Cambridge, England	6.0 cm	38,000
Armstrong and Sramek (1982)	VLA, New Mexico	6.1 cm	84,000
Basart et al. (1970)	Green Bank, West Virginia	11.1 cm	180,000

From Equation A24 it can be seen that r_o varies as $\lambda^{6/5}$, so we can compare the optical and radio data. The median values of r_o given in Table B-I are plotted in Figure B-1 as a function of wavelength. Superimposed on the data are two solid lines which represent very good seeing (nighttime mountain-top site), where

$$r_o(m) = 1000[\lambda(mm)]^{6/5} \qquad (B1)$$

and poor seeing (daytime low-altitude site), where

$$r_o(m) = 250[\lambda(mm)]^{6/5} \ . \qquad (B2)$$

The median data in Table B-I lie between these two lines. It can be seen that the agreement of the optical and radio data under similar conditions is generally better than a factor of two. Furthermore, since atmospheric absorption has essentially no effect on r_o, the two solid lines in Figure B-1 bracket the conditions to be expected at intermediate (sub-mm and far infrared) wavelengths. It should be emphasized that Equations B1 and B2 are strictly valid only if the integrated square of the refractive index structure parameter is independent of wavelength. The simplest theory is for dry air only and a wavelength-independent refractive index, and does not include the effects of humidity variations. These humidity variations will cause "extra" phase fluctuations at radio wavelengths, but their spatial and temporal spectra are of the Kolmogoroff type (Friehe et al. 1975) and therefore will be difficult to separate statistically from the dry air (i.e., temperature-driven) refractivity

fluctuations. Perhaps simultaneous multi-wavelength phase or refractivity measurements at the same site would allow separation of the "dry" and "wet" components. If the humidity fluctuations cause Cn^2 for radio wavelengths to be increased by a typical factor of 10 in the lowest 4 km of atmosphere, we expect r_0 from Equation A24 to be ~2.5 times smaller than predicted from the "dry air" turbulence alone. This factor is comparable to the site and diurnal variations and cannot at present be separated with certainty. In addition, in some conditions the negative covariance of temperature and humidity mitigates the larger phase fluctuations due to humidity at radio wavelengths. This effect may partially explain the good agreement between the optical and the radio data on Figure B-1. At the extremely long ground-based baselines ($> 10^6$ m) the atmospheric phase noise becomes decorrelated and ceases to increase with increasing baseline, thereby allowing successful VLBI observations.

The dashed lines in Figure B-1 represent the long-exposure image width θ_0. At optical wavelengths the best median value is about 1", but at 10 cm wavelength the median image size is almost 0.1". Thus ground-based radio interferometer arrays can produce higher resolution pictures than optical photographs also taken from the ground. At present this capability is limited to rather small fields of view, however, in reasonable observing times.

B2. OPTIMUM MILLIMETER AND SUB-MILLIMETER ARRAY SIZES

There is now considerable interest in constructing ground-based imaging arrays for use at millimeter (NRAO) and sub-millimeter (SAO) wavelengths. In this section we predict the maximum useful array sizes. If we choose 1

FIGURE B-1

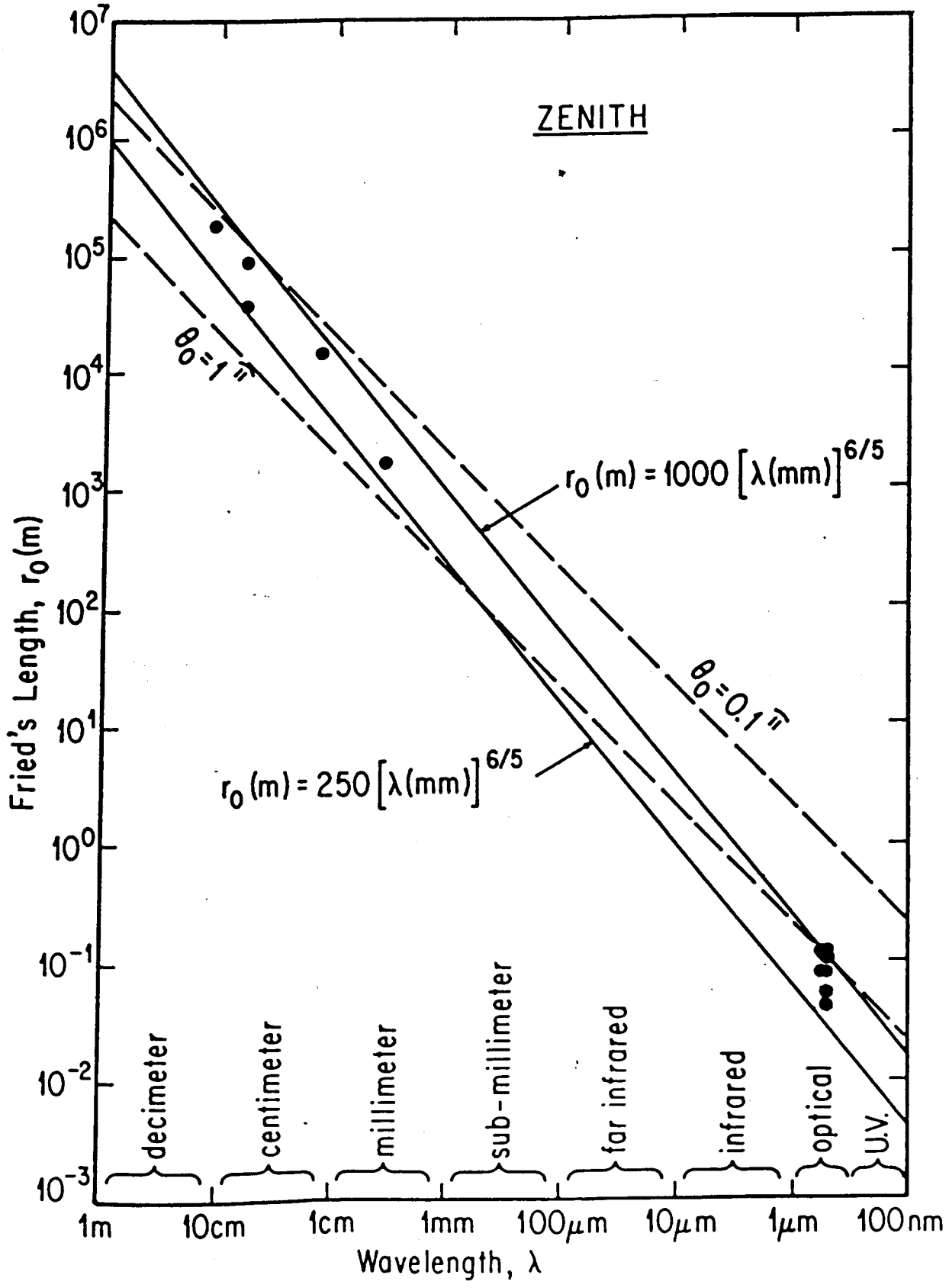
ZENITH
r_0 (m) = 1000 [λ(mm)]$^{6/5}$
r_0 (m) = 250 [λ(mm)]$^{6/5}$
θ_0=1"
θ_0=0.1"
Fried's Length, r_0(m)
10^7
10^6
10^5
10^4
10^3
10^2
10^1
10^0
10^{-1}
10^{-2}
10^{-3}
decimeter
centimeter
millimeter
sub-millimeter
far infrared
infrared
optical
U.V.
1m
10cm
1cm
1mm
100μm
10μm
1μm
100nm
Wavelength, λ

radian R.M.S. as the maximum useful phase error from one end of the maximum projected baseline B to the other end, we find from Equations A27 and A41 that

$$B = 0.315\, r_0 A^{-3/5} \tag{B3}$$

where r_0 refers to the zenith value. Thus, combining Equations B3 and B1 we find that under very good seeing conditions the maximum useful baseline B is given by

$$B = 315[\lambda(mm)]^{6/5} A^{-3/5}\ (m) \tag{B4}$$

and with poor seeing

$$B = 79[\lambda(mm)]^{6/5} A^{-3/5} (m)\ . \tag{B5}$$

Table B-II presents median values of B for the three useful observing wavelengths of 2.6 mm, 1.0 mm, and 0.35 mm. The $B_{1\sigma}$ values also listed in Table B-II refer to the minimum useful baselines for 18% of the best time. Only 18% of the time will the atmosphere allow useful observing over longer baselines, and 82% of the time the atmosphere will allow only shorter baselines to be effectively used.

Sites with very good seeing (Mt. Graham, Mt. Lemmon, or Mauna Kea) will allow array baselines up to 920 m, 290 m, and 83 m at 2.6 mm, 1.0 mm, and 0.35 mm wavelength respectively, down to 30^{o} elevation angle during the best 18 % of the time. From Figure B-1 we can see that the VLA site has moderately good seeing, and the useful array sizes will be about two-thirds of the sizes possible at the very best developed high-altitude sites.

TABLE B-II

MAXIMUM USEFUL ARRAY BASELINES

Wavelength (mm)	2.6	1.0	0.35
I. VERY GOOD SEEING			
$\langle r_o \rangle$ (m)	3148	1000	284
$\langle B \rangle$ (m), A = 1	991	315	89
$\langle B \rangle$ (m), A = 2	654	208	59
$B_{1\sigma}$ (m), A = 1	1390	440	125
$B_{1\sigma}$ (m), A = 2	920	290	83
II. POOR SEEING			
$\langle r_o \rangle$ (m)	787	250	71
$\langle B \rangle$ (m), A = 1	249	79	22
$\langle B \rangle$ (m), A = 2	164	52	15
$B_{1\sigma}$ (m), A = 1	350	111	31
$B_{1\sigma}$ (m), A = 2	230	73	21

APPENDIX REFERENCES

Allen, C. W. 1963, Astrophysical Quantities, Athlone, London, 119-120.

Armand, N. A., Izyumov, A. O., and Sokolov, A. V. 1971, Radio Engr. Electron. Phys. 16, 1259-1266.

Armstrong, J. W. and Sramek, R. A. 1982, Radio Science 17, 1579-1586.

Barletti, R., Ceppatelli, G., Paterno, L., Righini, A., and Speroni, N. 1977, Astron. Astrophys. 54, 649-659.

Basart, J. P., Miley, G. K., and Clark, B. G. 1970, IEEE Trans. Antennas Propagat. AP-18, 375-379.

Bean, B. R. 1962, Proc. IRE 50, 260-273.

Bieging, J. H., Morgan, J., Welch, W. J., Vogel, S. N., and Wright, M. C. H. 1984, submitted to Radio Science.

Boyd, R. W. 1978, J. Opt. Soc. Am. 68, 877-883.

Clifford, S. F. and Strohbehn, J. W. 1970, IEEE Trans. Antennas Propagat. AP-18, 267-274.

Cole, R. S., Ho, K. L., and Mavrokoukoulakis, N. P. 1978, IEEE Trans. Antennas Propagat. AP-26, 712-715.

Dainty, J. C. and Scaddan, R. J. 1975, Mon. Not. R. Astr. Soc. 170, 519-532.

Fante, R. L. 1980, Proc. IEEE 68, 1424-1443.

Filho, F. C. Medeiros, Jayasuriya, A. R., Cole, R. S., and Helmis, C. G. 1983, IEEE Trans. Antennas Propagat. AP-31, 672-676.

Fried, D. L. 1965, J. Opt. Soc. Am. 55, 1427-1435 (errata in Fried, D. L. 1966, J. Opt. Soc. Am. 56, 410).

Fried, D. L. 1966, J. Opt. Soc. Am. 56, 1372-1379.

Fried, D. L. 1967a, Proc. IEEE 55, 57-67.

Fried, D. L. 1967b, J. Opt. Soc. Am. 57, 175-180.

Fried, D. L. 1977, Appl. Opt. 16, 549.

Fried, D. L. and Mevers, G. E. 1974, Appl. Opt. 13, 2620-2622.

Friehe, C. A., La Rue, J. C., Champagne, F. H., Gibson, C. H., and Dreyer, G. F. 1975, J. Opt. Soc. Am. 65, 1502-1511.

Greenwood, D. P. and Fried, D. L. 1976, J. Opt. Soc. Am. 66, 193-206.

Gurvich, A. S. 1968, Radio Engr. Electron. Phys. 13, 1687-1694.

Gur'yanov, A. E. 1980, Sov. Astron. 24, 379-383.

Hill, R. J. 1978, Radio Science 13, 953-961.

Hinder, R. A. 1970, Nature 225, 614-617.

Hogg, D. C., Guiraud, F. O., and Decker, M. T. 1981, Astron. Astrophys. 95, 304-307.

Izyumov, A. O. 1968, Radio Engr. Electron. Phys. 13, 1009-1013.

Johnson, C. B. 1973, Appl. Opt. 12, 1031-1033.

Kolmogoroff, A. 1961, Turbulence, Classic Papers on Statistical Theory, ed. by S. K. Friedlander and L. Topper, Interscience, New York, 151.

Liebe, H. J. and Hopponen, J. D. 1977, IEEE Trans. Antennas Propagat. AP-25, 336-345.

Loos, G. C. and Hogge, C. B. 1979, Appl. Opt. 18, 2654-2661.

Miller, M. G. and Zieske, P. L. 1977, J. Opt. Soc. Am. 67, 1680-1685.

Ott, R. H. and Thompson, M. C., Jr. 1978, IEEE Trans. Antennas Propagat. AP-26, 329-332.

Pandey, P. C. and Kakar, R. K. 1983, IEEE Trans. Antennas Propagat. AP-31, 136-140.

Pollaine, S., Buffington, A., and Crawford, F. S. 1979, J. Opt. Soc. Am. 69, 84-89.

Roddier, F. 1981, Progress in Optics XIX, ed. by E. Wolf, ch. 5, North Holland, New York, 282-376.

Smith, E. K., Jr. and Weintraub, S. 1953, Proc. IRE 41, 1035-1037.

Sramek, R. 1983, National Radio Astronomy Observatory VLA Test Memo 143.

Sutton, E. C., Subramanian, S., and Townes, C. H. 1982, Astron. Astrophys. 110, 324-331.

Tatarskii, V. I. 1971, The Effects of the Turbulent Atmosphere on Wave Propagation, Israel Program for Scientific Translation, Jerusalem.

Thompson, M. C., Jr., Marler, F. E., and Allen, K. C. 1980, IEEE Trans. Antennas Propagat. AP-28, 278-280.

Ulich, B. L. 1984, in preparation.

Walters, D. L. 1981, J. Opt. Soc. Am. 71, 406-409.

Walters, D. L. and Kunkel, K. E. 1981, J. Opt. Soc. Am. 71, 397-405.

Walters, D. L., Favier, D. L., and Hines, J. R. 1979, J. Opt. Soc. Am. 69, 828-837.

Woolf, N. J. 1982, Ann. Rev. Astron. Astrophys. 20, 367-398.

Wyngaard, J. C., Pennell, W. T., Lenschow, D. H., and LeMone, M. A. 1978, J. Atmos. Sci. 35, 47-58.

Young, A. T. 1974, Ap. J. 189, 587-604.